Published in final edited form as:
J Biomed Nanotechnol. 2021 June 01; 17(6): 1170–1183. doi:10.1166/jbn.2021.3091.

Pulsed Focal Ultrasound as a Non-Invasive Method to Deliver Exosomes in the Brain/Stroke

Ahmet Alptekin[1], **Mohammad B. Khan**[2], **Roxan Ara**[1], **Mohammad H. Rashid**[1], **Fengchong Kong**[1], **Mahrima Parvin**[1], **Joseph A. Frank**[3,6], **Rajiv Chopra**[4], **Krishnan Dhandapani**[5], **Ali S. Arbab**[1,*]

[1]Georgia Cancer Center, Augusta University, Augusta, GA

[2]Department of Neurology, Augusta University, Augusta, GA

[3]Frank Laboratory, Radiology and Imaging Science, Clinical Center, NIH, Bethesda, MD

[4]Department of Radiology and Advanced Imaging Research Center, UT Southwestern Medical Center, Dallas, TX

[5]Department of Neurosurgery, Augusta University, Augusta, GA

[6]National Institute of Biomedical Imaging and Bioengineering, NIH, Bethesda, MD

Abstract

Exosomes, a component of extracellular vesicles, are shown to carry important small RNAs, mRNAs, protein, and bioactive lipid from parent cells and are found in most biological fluids. Investigators have demonstrated the importance of mesenchymal stem cells derived exosomes in repairing stroke lesions. However, exosomes from endothelial progenitor cells have not been tested in any stroke model, nor has there been an evaluation of whether these exosomes target/home to areas of pathology. Targeted delivery of intravenous administered exosomes has been a great challenge, and a targeted delivery system is lacking to deliver naïve *(unmodified)* exosomes from endothelial progenitor cells to the site of interest. Pulsed focused ultrasound is being used for therapeutic and experimental purposes. There has not been any report showing the use of low-intensity pulsed focused ultrasound to deliver exosomes to the site of interest in stroke models. In this proof of principle study, we have shown different parameters of pulsed focused ultrasound to deliver exosomes in the intact and stroke brain with or without intravenous administration of nanobubbles. The study results showed that administration of nanobubbles is detrimental to the brain structures (micro bleeding and white matter destruction) at peak negative pressure of >0.25 megapascal, despite enhanced delivery of intravenous administered exosomes. However, without

*Author to whom correspondence should be addressed. aarbab@augusta.edu.

Conflicts of Interest

Dr. Rajiv Chopra is co-founder of FUS Instruments.

Ethics Compliance

All experiments were performed according to the National Institutes of Health (NIH) guidelines. The Institutional Animal Care and Use Committee (IACUC) of Augusta University approved all the experimental procedures (protocol #2014–0625). Animals were kept under regular barrier conditions at room temperature with exposure to light for 12 hours and dark for 12 hours. Food and water were provided ad libitum. All required efforts were made to ameliorate the suffering of animals. CO2 with a secondary method was used to euthanize animals for tissue collection. A minimum of 4 animals was included in each experimental group.

nanobubbles, pulsed focused ultrasound enhances the delivery of exosomes in the stroke area without altering the brain structures.

Keywords

Pulsed Focal Ultrasound; Brain; Stroke; Exosomes Delivery; Magnetic Resonance Imaging

INTRODUCTION

Exosomes are 30–150 nm lipid bi-layered extracellular bioactive vesicles of endosomal origin that are secreted by all cells and present in various body fluids. The exosomal content is released by the fusion of these endosomes with the plasma membrane [1]. Exosomes contain lipids, proteins, DNA, RNA, and various metabolites from origin cells [2]. Their stability in the extracellular environment, ability to carry a payload, and specificity to tissues and organs got attention to the use of exosomes as a vehicle to deliver drugs and other treatments to target sites in the body, including the brain [3–6]. Exosomes have been used for therapeutic purposes to target stroke and other disorders [7, 8]. Investigators have shown the importance of mesenchymal stem cells (MSCs) derived exosomes in repairing stroke lesions [9]. Repeated administration of exosomes in the rat subjected to the “mechanical occluded” stroke model showed improved functionality and reduced stroke injury [9, 10]. Targeted delivery of intravenous (IV) administered exosomes has been a great challenge, especially through blood-brain-barrier (BBB). Modification of exosomal surface to carry different ligands or peptides have been tried to increase delivery to target tissues [11, 12]. However, the overall results were not encouraging [13, 14]. Investigators are trying to deliver naïve exosomes without surface modification for optimal effect [15]. Delivery of exosomes to the brain is a daunting task, and BBB penetrable peptides have been considered [16, 17]. Targeted delivery systems are lacking to *deliver naïve (unmodified)* exosomes to the site of interest, especially in the brain or in the area of stroke.

The BBB consists of endothelial and neuronal cells, and it prevents most of the blood content from reaching the brain, including most of the drugs and exosomes. Different osmotic and chemical techniques have been developed to overcome BBB with various successes, as well as physical disruption by ultrasound. Therapeutic ultrasound delivers mechanical forces that, when coupled with ultrasound contrast agent microbubbles/nanobubbles, can disrupt the BBB and enhances permeability [18]. Moreover, ultrasound contrast agents such as micro/nanobubbles intensify this acoustic force in the vessels and amplify the effect of ultrasound. Ultrasound alone or in combination with micro/nanobubbles have been used to open BBB [19–22] and facilitated the delivery of drugs [23, 24], immunoglobulins [25], albumin [26], and antibodies [27] to the brain.

The aim of the study was to test and optimize the parameters of pulsed focused ultrasound (pFUS) with or without nanobubbles to transiently disrupt BBB to enhance the accumulation of IV administered exosomes in the area of interest without damaging the brain parenchyma. The relatively optimized pFUS were then applied to deliver exosomes to lesions in a mouse with transient middle cerebral artery occlusion (MCAO) mediated stroke model.

MATERIALS AND METHODS

Chemicals and Antibodies

All chemicals and antibodies used in the studies were bought from reputed commercial vendors. Anti-albumin (A0353, ABClonal) and FITC-conjugated AffiniPure Goat Anti-Rabbit (111–095-003, Jackson Laboratories) were used to determine the leakage of BBB. Luxol Fast Blue (#212170250, Acros Organics) used to assess the integrity of white matters, Prussian Blue Stain kit (#3160, Eng Scientific) was used to detect micro bleeding in the brain. HEK293 cells were acquired from ATCC, and mouse endothelial progenitor cells (EPC) were collected from the bone marrow of mice using a magnetic sorter as per our previous methods [28]. CellTracker™ CM-DiI (C7000, Thermo Fisher) lipophilic fluorescent dye was purchased for exosome labeling. Fluorescent (FITC) tagged tomato lectin was used to outline the blood vessels (DL-1174, Vector Labs).

Preclinical Bench-Top Focused Ultrasound System (RK-50)

The RK-50 (FUS Instruments Inc, Canada) is a standalone preclinical focused ultrasound system designed for large throughput blood-brain barrier experiments. Atlas-based targeting combined with an optional multi-modality high field insert allows the system to be used with or without magnetic resonance imaging (MRI) or X-ray computed tomography (CT) guidance and imaging. The system is based upon a flexible cross-platform animal handling system simplifying handling and increasing efficiency. The instrument has a three-axis motorized positioning system and an accurate stereotaxic-guided targeting system that uses rodent brain atlases (mouse and rat). It has a calibrated spherically focused ultrasound transducer (typically 1.47 MHz) with a maximum radio frequency power of 15 Watt and includes animal restraint and inhalant anesthetic fixtures. It also has custom-written software for atlas registration and treatment planning capability to deliver single or multi-point acoustic exposures (continuous or pulsed).

Nanobubbles and Characterization

Nanobubbles as ultra-sonogram contrast agents were purchased from FUS Instruments Inc. (Toronto, Canada) and prepared according to the supplied protocol. In brief, the unmixed vial was placed in a vial mixture and shaken at 4500 rpm for 5 minutes to make activated emulsion (nanobubbles) containing gas. Then the vial was centrifuged upside down at 800 rpm for 5 minutes. Following centrifugation, the solution containing emulsion of nanobubbles was drawn into a 1 ml insulin syringe without disturbing the foamy upper part. Following activation of nanobubbles, the size and zeta potential of the nanobubbles were determined by a nanoparticle tracking analyzer (NTA). The nanobubbles were diluted 1:1 ratio using sterile PBS before injecting into the tail vein of the mice.

Parameters of Pulsed Focal Ultrasound (PFUS) in Normal Brain

We reviewed previous studies (Table I) and set up our parameters. All experiments were performed using a 1.47 Megahertz (MHz) (frequency) focal (concave) transducer (wavelength of 1.047 mm). Pulsed ultrasound was applied to 5 points in and around the bregma (at 3 mm lateral from the midline and 3.5 mm deep from the surface on both sides of

the brain, with 1% duty cycle (burst duration of 10 milliseconds (ms), repetition period 1000 ms), for 90 to 180 burst. We have used 0.25 to 2 Megapascal (MPa) amplitude of pressure (acoustic power) to the tissue with or without nanobubbles to determine the changes in the BBB and the damages to the structures of the brain tissues. Animals received 0.5 to 2 MPa pFUS to one hemisphere of the brain. After completing pFUS without nanobubbles on one hemisphere (right hemisphere), nanobubbles were administered by IV, and 0.25 to 1 MPa pFUS given to the contralateral side of the brain (left hemisphere).

Preparation of Animals

We have used 6–8 weeks old immunocompetent Balb/c mice (both males and females) as well as 8–10 months old C57BL/6 mice with stroke (24 hours after MCAO). Following gas anesthesia with aseptic techniques, a midline incision was made on the scalp to expose and register bregma and lambda points. With the help of a mouse brain atlas, we have selected a central point at 3 mm lateral to bregma and 3.5 mm deep in the brain tissue and then set four more points at 2 mm apart from the central point (left, right, front, and back). Then desired pFUS was applied with or without IV nanobubbles administration. Following pFUS, the skin wound was sutured, and the animals were allowed to recover. When applicable, before or soon after the completion of pFUS, DiI labeled exosomes were IV administered to determine the distribution of exosomes in the normal and pFUS irradiated areas.

Collection of EPC Exosomes and DiI Labeling

Endothelial progenitor cells collected from the bone marrow of Balb/c mice using c-kit positive selection kit (8802–6838-74, ThermoFisher) according to manufacturers' protocol. EPC exosomes were collected from the culture media as per our published method [40]. 12×10^9 EPC-derived exosomes in 1 ml PBS incubated with 5 μl DiI fluorescent dye at 37 °C for 10 minutes and then followed by an incubation at 4 °C for 20 minutes. Labeled exosomes washed by adding 1 ml PBS and centrifugation with 30k centrifugal filter (UFC4 LTK 25, Amicon) for 30 minutes at 3900 RPM. After a second wash, exosomes were suspended in 0.6 ml volume of PBS. The size of the exosomes is shown in Figure 1.

Immunohistochemistry

Luxol fast blue staining was done to determine the integrity of white matter. Staining for extravasated albumin was done to determine the leakage of BBB. Staining for blood vessels was done by FITC-tagged tomato lectin. These stainings were done according to the manufacturer's protocol. Micro bleeding in the brain was determined by DAB enhanced Prussian blue staining as per our published protocols [41]. To evaluate the tissue integrity, hematoxylin and eosin staining were used.

Magnetic Resonance Imaging (MRI)

A 7 T dedicated small animal MRI system was used to acquire all the MR images (BioSpec 70/20 USR, Bruker). Animals underwent MRI soon after (within 60 minutes) and at 24 hours following pFUS experiments. To determine the edema formation, T2-weighted and multislice-multi-echo (MSME) T2 images were acquired, followed by the creation of T2-maps. To determine BBB leakage, animals received IP injection of Gadolinium-DTPA

contrast agent, and T1-weighted images were acquired. Following the last MRI at 24 hrs, animals were euthanized, perfused, and the brains were collected and fixed for further histochemical studies.

Making of Stroke Model, MRI, and PFUS in the Stroke Areas

Briefly, anesthetized mice have undergone a midline incision on the ventral side of the neck. Then, the right common carotid artery (CCA), the right external carotid artery (ECA), and the right internal carotid artery (ICA) were assessed [42]. Based on the body weight, a silicone rubber-coated monofilament suture (Doccol Corp) was introduced into the ECA lumen and advanced into the ICA until a slight resistance is felt to occlude the origin of the middle cerebral artery (MCA). At 60-min post-occlusion, the filament was gently withdrawn to reinstate cerebral blood flow (CBF) in large vessels as determined with laser speckle imager as described previously [43]. All animals underwent MRI 24 hrs after stroke to determine the region and extent of the stroke areas. Based on the MR images, 10 points from trans axial sections of the stroke area were selected for pFUS (from 0.5 to 2 MPa) to facilitate the delivery of exosomes in randomly chosen animals. 90 burst of pFUS applied sequentially to 10 points and then 3×10^9 EPC exosome IV administered. All stroke animals were euthanized after 3 hours of IV injection of DiI labeled exosomes, perfused with PBS, and the brains harvested to determine the accumulation of exosomes.

Optical Images of *Ex Vivo* Brain

To determine the accumulation of DiI labeled exosomes in stroke area with or without pFUS at different peak negative pressure (0.5, 1.0, 2.0 MPa), collected intact brain underwent fluorescent imaging using optimal excitation and emission wavelength. Then the photon intensity was determined from the right and left hemispheres of each brain and the intensity ratio was calculated (right hemisphere photon intensity/left hemisphere photon intensity). The ratio was compared among all the conditions.

Statistical Analysis

Quantitative data presented in this research were expressed as mean ± standard deviation unless otherwise stated. Statistical differences between more than two groups were determined by analysis of variance (ANOVA) followed by multiple comparisons using Tukey's multiple comparisons test. Comparison between 2 samples was performed by Student t-test. GraphPad Prism version 8.2.1 for Windows (GraphPad Software, Inc., San Diego, CA) was used to perform the statistical analysis. Differences with p-values less than 0.05 were considered significant (*p <05, **p < 01, ***p < 001, ****p < 0001).

RESULTS

BBB Leakage Observed on MRI

Characteristics of nanobubbles are shown in Figure 2. The size of the nanobubbles was 173.6 (±85.4) nm with a zeta potential of −29.10±2.10 mV. To determine the effect of applied pFUS peak negative pressure (PNP) and BBB leakage with or without nanobubbles, animals underwent post-contrast T1-weighted MRI 1 hour and 24 hrs after pFUS. Using a stereotactic-guided focused ultrasound device, we tested different pFUS PNP to find

the maximum non-disruptive dose. We applied pFUS to the right hemisphere without nanobubbles first and then applied pFUS to the left hemisphere during the infusion of nanobubbles. pFUS parameters were consisted of 180 cycles, with 10 ms burst and 1000 ms pulse repetition time of each cycle. The pFUS dose ranges from 0.5 to 2 MPa without nanobubbles did not cause any BBB leakage indicated by non-enhancement at the site of pFUS in the right hemisphere (Figs. 3(A)–(C)).

On the other hand, 1 hour MRI images showed BBB leakage at the site of pFUS with nanobubbles even at the lowest dose of 0.25 MPa, although the leakage at 0.25 MPa was transient as no enhancement was observed on 24-hour postcontrast MRI (Fig. 3(A)). pFUS doses with nanobubbles at 0.5 and 1 MPa showed sustained BBB leakage, which was observed on 24 hour MRI as contrast-enhanced areas on the left hemisphere (Figs. 3(B)–(C), left hemispheres). A significant advantage of using nanobubbles was observed for opening BBB, even with the lowest dose applied. We also observed a decrease in the signal intensity following contrast administration on MRI at 24 hrs in animals that received 0.5 MPa and 1 MPa pFUS with nanobubbles (Figs. 3(B), (C)), which might indicate a gradual repair of BBB leakage.

Damage of Intact Brain Following PFUS

To evaluate tissue damage and bleeding after pFUS application, we sacrificed all animals after 24 hours of pFUS, and harvested brain tissue, fixed it with paraformaldehyde, and made paraffin blocks to make sections for different IHC analysis. We stained tissues with luxol fast blue (LFB) and Prussian blue to evaluate the damage to white matter (myelin sheath) and bleeding, respectively. LFB staining showed damage to the myelin sheath or white matter, starting with 0.5 MPa pFUS when nanobubbles were used (Figs. 4(B)–(C), left). However, we did not observe similar damage to the white matter even with 2 MPa pFUS when nanobubbles were not used (Figs. 4(A)–(C), right). Similar to the damage of white matters, micro bleeding (DAB enhanced Prussian blue staining, brown spots) was also observed in the pFUS irradiated area (both at 0.5 and 1 MPa) when nanobubbles were used (Figs. 5(B)–(C), left). On the other hand, no micro bleeding was observed even with the highest pFUS (at 2 MPa) without nanobubbles (Figs. 5(A)–(C), right). These findings, in combination with MRI findings, indicate that 0.25 MPa with nanobubbles opens BBB without causing structural damage or bleeding, but using pFUS PNP >0.5 MPa with nanobubbles causes structural damage to the intact brain with the parameters described above. However, pFUS without nanobubbles is safe even with the highest applied 2 MPa intensity.

Confirmation of BBB Opening

Albumin is a plasma protein, and its leakage into brain parenchyma indicates a BBB opening [44]. To investigate albumin leakage, we stained the paraffin sections with FITC-anti-albumin antibody. Leakage of albumin (labeling FITC-tagged anti-albumin antibody) was observed when pFUS was used following IV administration of nanobubbles only in cases where pFUS intensity was at 1 MPa and 0.5 MPa (Figs. 6(A)–(C), left). However, we have not observed any leakage of albumin following irradiation up to 2 MPa pFUS without

nanobubbles (Figs. 6(A)–(C), right). Corresponding HE staining showed preserved tissue integrity in the area of albumin leakage following pFUS with nanobubbles (Fig. 7).

Exosome Delivery into the Brain in the Stroke Model

In a cerebral stroke, the BBB is already compromised. Our previous studies showed the accumulation of neural stem cells (NSC) derived exosomes in the stroke areas without the application of pFUS [45]. Because the stroke already resulted in damage to the BBB and parenchyma, further disruption with nanobubbles addition would be detrimental and therefore nanobubbles were not infused. We wanted to see whether the application of pFUS without nanobubbles will enhance the accumulation of IV administered exosomes in the stroke areas. We used the right middle cerebral artery occlusion (MCAO) as a stroke model in mice. 24 hours after stroke, we obtained MRI (Figs. 8(A)–(C), middle). After determining the stroke area, we applied 0.5 MPa (Fig. 8(A)), 1 MPa (Fig. 8(B)), and 2 MPa (Fig. 8(C)) pFUS to 10 selected points in the stroke area to induce BBB opening and administered DiI-labeled EPC-derived exosomes via IV injection. A second IV dose of exosomes was administered the next day following pFUS, and brains were harvested 3 hours following 2nd dose of exosomes. We found the accumulation of exosomes was enhanced when pFUS was applied at the area around the stroke sites (Figs. 8(A)–(C); right) compared to corresponding sections in the contralateral side of the brain (Figs. 8(A)–(C); left). We also observed significantly ($p < 001$) increased exosome delivery in animals that received pFUS at PNP of 1 MPa and 2 MPa pFUS application, compared to 0.5 MPa. The number of exosomes in respect of the total area of pixels was determined by the color threshold method using ImageJ. 2 MPa PNP showed the total area of exosomes (0.12±0.03) versus (0.02±0.03) for 0.5 MPa. 1 MPa showed (0.10±0.10) area of exosomes. These findings indicate that pFUS without nanobubbles improves the exosome delivery and that pFUS could be used to induce the delivery of exosomes into brain parenchyma. Photon intensity analysis from optical imaging also showed increased accumulation of DiI-labeled EPC exosomes in the stroke area (right hemisphere) that received pFUS at 2 MPa (Fig. 9).

We checked whether the exosomes are attached to the endothelial lining or extravasated and accumulated in the brain parenchyma. Sections were stained with FITC tagged tomato lectin to delineate the endothelial lining in the area of exosome accumulation. Although the exosomes were found inside the vessel, high-resolution images showed the accumulation of exosomes in the deeper part of the brain parenchyma away from the endothelial lining. This finding indicates blood vessels' opening to allow the exosomes' accumulation into the brain (Fig. 10).

Discussion and Notes

The study's purpose was to determine the safe pFUS parameters to deliver the naïve exosomes at the stroke site. Our studies clearly showed that pFUS at PNP of 1 to 2 MPa could enhance the delivery of naïve intravenously administered exosomes to the stroke areas. Many studies have utilized pFUS to deliver nanoparticles or other agents at irradiation sites with or without administration of nano/microbubbles [46]. Previous studies showed enhanced delivery of nanoparticles into intact brain parenchyma when pFUS was used [47]. However, none has used the technique to deliver exosomes to the site of a stroke. It is

known that BBB is already open at the site of stroke [48], which may preclude the use of nano/microbubbles during pFUS. The use of nano/microbubbles may be detrimental to the stroke area. Moreover, the stroke area showed extensive inflammatory processes due to the accumulation of neutrophils and other inflammatory cells [49], therefore causing more inflammation may not be the desired outcome following pFUS mediated injury [26].

The current stroke treatment is thrombolysis in the stroke's acute phase [50]. However, more treatment options and safe delivery of therapeutics into brain parenchyma are needed. One strategy is to deliver stem cell-derived extracellular vesicles to facilitate the repair or stimulate the replacement of the infarcted tissue. It has been shown that there was no difference in recovery after ischemic stroke in mice following the infusion of mesenchymal stem cells (MSC) as compared to extracellular vesicles derived from the MSC [51]. Another study demonstrated extracellular vesicles from MSC improved recovery of stroke in rat models [52]. Previously, we have reported that extracellular vesicles from human neural stem cells improved the recovery in a stroke model in mice [45]. Taken together, these studies demonstrate that exosomes could be a novel therapeutic in the treatment of stroke. However, all of the studies mentioned above relied on the passive distribution and accumulation of exosomes at the penumbra or peristroke regions.

While the BBB is responsible for excluding large molecules, it can allow the transport of small lipophilic molecules (<400–500 Da) [53]. This makes the brain an organ, which is hard to reach for most drugs, including most of the exosomes. Among different strategies to overcome BBB to reach the brain parenchyma, it has been demonstrated that pFUS mechanical forces can disrupt and open BBB without permanent damage to brain parenchyma in rodents [22]. By optimizing this technique with microbubbles and employing MRI guidance, researchers successfully opened the BBB in patients with Alzheimer's [54] and amyotrophic lateral sclerosis [19]. It has also been demonstrated that magnetic resonance-guided pFUS with microbubbles resulted in BBB opening in glioma patients and increased delivery of chemotherapeutics [55]. To date, chemotherapy agents, antibodies, gene therapy agents, nanoparticles, and cells were able to be transferred to the brain with the help of pFUS coupled with microbubbles infusion [56].

In the treatment of stroke, therapeutic ultrasound (sonothrombolysis) has been tested as an adjunctive to tPA therapy. Although it was found to be safe, there was no clinical benefit in stroke patients [57]. There is presently an ongoing phase 2 clinical study that is investigating the use of therapeutic ultrasound in combination with microbubble infusion (NCT01678495). Besides these thrombolytic approaches in stroke, other studies have employed therapeutic ultrasound to deliver therapeutic agents to brain parenchyma. Previous studies showed that enhanced delivery of nanoparticles in the brain parenchyma and in the tumor areas when pFUS was applied without any microbubbles. This enhanced delivery was due to the lowering of interstitial pressure [47, 58].

The transient nature of BBB opening was also observed following low-intensity pFUS + microbubbles, and it has been reported that the BBB closes at 28 [38], 24 [32], and 8 hours [29]. This indicates that pFUS does not cause permanent damage and can temporarily open BBB for therapeutic delivery in the intact brain. Clinical trials demonstrated that

ultrasound-induced BBB opening was closed after 24 hours and proved its safety in humans to be used in therapeutic delivery into the brain [54]. Based on our findings, pFUS at 0.25 MPa with nanobubbles can be used to open BBB and deliver exosomes without damaging the brain structures.

However, our aim was to increase the delivery of exosomes in the stroke area without nanobubbles administration. It is already known that BBB is already open in a stroke area [48]. Therefore, we tried to find the best possible parameters to deliver naïve IV administered exosomes to the stroke site without destructing the brain structures. As our results showed no detrimental effects in the intact brain, we have used pFUS with 0.5 to 2 MPa intensities without nanobubbles. Our results indicated any intensities above 0.5 MPa would allow enhanced naïve IV administered exosomes in the stroke areas away from the endothelial lining. We are now investigating EPC-derived exosomes' effect on stroke outcomes. It is already known that stroke would increase the leakage of BBB and exosomes should be accumulated freely in the stroke area once IV is administered. However, significantly increased accumulation following PNP >0.5 MPa indicated a synergistic effect that may open up BBB further or cause transient increased inflammatory cascades that allowed adherence of IV administered EPC-derived exosomes. In recent publications, investigators have pointed out transient sterile inflammation in the brain following pFUS [26, 39].

Fluorescent imaging of the mouse brain to detect DiI-labeled exosome showed an increased signal on the right hemisphere compared to the left, but it was not statistically significant (borderline significance was observed ($p = 006$) when compared with non-irradiated versus PNP 2 MPa irradiated stroke area). This non-significant photon intensity could be due to our method of analysis. Because we measure the photon intensity from the whole hemisphere (both left and right), which included stroke areas (right hemisphere) without blood supply and delivery of exosomes, the photon intensity was averaged out. The photon intensity in the right hemisphere could be higher if we could exclude the stroke areas. However, we found an increased exosome presence around the stroke area compared to the stroke core, indicating the exosome extravasation is more in the penumbra area. We continue to investigate this part of the study using more animals with immunofluorescence studies. We also found that even without pFUS application, exosome delivery to the right hemisphere (stroke side) was increased compared to that of the left hemisphere. This finding confirms that EPC exosome delivery is also increased stroke lesions.

Limitation of the Studies

We have not studied the expression of different cytokines following different doses of pFUS. Previous studies showed sterile inflammatory response following pFUS in the brain parenchyma [26]. However, it is already known that stroke caused a massive inflammatory reaction. We will investigate inflammatory cytokines using membrane array or proteomics in the stroke areas with or without pFUS in our future studies. It is also known that higher PNP can cause heating of the skull at the irradiation site [59]. Moreover, local heating may cause exosome accumulation under the skull rather than inside the brain parenchyma. However, our IHC analysis showed an accumulation of exosomes in the deeper part of the

brain parenchyma. Ultrasound may alter the neurobehaviour of the animals [60]. Our next sets of studies are looking at the neurobehaviour of animals following pFUS with or without EPC exosomes. The results are forthcoming.

CONCLUSION

pFUS without micro/nanobubbles can be used to deliver IV administered exosomes to the site of interest. Engineered or non-engineered exosomes can be used as therapeutics for stroke therapy in addition to tPA.

Acknowledgments:

The study was funded by American Heart Associate (AHA) grant 19TPA34850076 and part of Georgia Cancer Center start-up fund to ASA, and NIH grant R01NS117565 to KD.

REFERENCES

1. Thery C, Zitvogel L and Amigorena S, 2002. Exosomes: Composition, biogenesis and function. Nature Reviews: Immunology, 2, pp.569–579.
2. Jeppesen DK, Fenix AM, Franklin JL, Higginbotham JN, Zhang Q, Zimmerman LJ, Liebler DC, Ping J, Liu Q, Evans R, Fissell WH, Patton JG, Rome LH, Burnette DT and Coffey RJ, 2019. Reassessment of exosome composition. Cell, 177, pp.428–445, e418. [PubMed: 30951670]
3. Man F, Wang J and Lu R, 2020. Techniques and applications of animal- and plant-derived exosome-based drug delivery system. Journal of Biomedical Nanotechnology, 16, pp.1543–1569. [PubMed: 33461649]
4. Feng J, Waqas A, Zhu Z and Chen L, 2020. Exosomes: Applications in respiratory infectious diseases and prospects for coronavirus disease 2019 (COVID-19). Journal of Biomedical Nanotechnology,. 16, pp.399–418. [PubMed: 32970974]
5. Xiong F, Ling X, Chen X, Chen J, Tan J, Cao W, Ge L, Ma M and Wu J, 2019. Pursuing specific chemotherapy of orthotopic breast cancer with lung metastasis from docking nanoparticles driven by bioinspired exosomes. Nano Letters,. 19, pp.3256–3266. [PubMed: 30965009]
6. Batrakova EV and Kim MS, 2015. Using exosomes, naturally-equipped nanocarriers, for drug delivery. Journal of Controlled Release,. 219, pp.396–405. [PubMed: 26241750]
7. Zhang ZG and Chopp M, 2016. Exosomes in stroke pathogenesis and therapy. Journal of Clinical Investigation,. 126, pp.1190–1197. [PubMed: 27035810]
8. Xin H, Li Y and Chopp M, 2014. Exosomes/miRNAs as mediating cell-based therapy of stroke. Frontiers in Cellular Neuroscience,. 8, article 377, pp 1–11. [PubMed: 24478626]
9. Xin H, Li Y, Cui Y, Yang JJ, Zhang ZG and Chopp M, 2013. Systemic administration of exosomes released from mesenchymal stromal cells promote functional recovery and neurovascular plasticity after stroke in rats. Journal of Cerebral Blood Flow and Metabolism,. 33, pp.1711–1715. [PubMed: 23963371]
10. Xin H, Li Y, Liu Z, Wang X, Shang X, Cui Y, Zhang ZG and Chopp M, 2013. Mir-133b promotes neural plasticity and functional recovery after treatment of stroke with multipotent mesenchymal stromal cells in rats via transfer of exosome-enriched extracellular particles. Stem Cells,. 31, pp.2737–2746. [PubMed: 23630198]
11. Stickney Z, Losacco J, Mcdevitt S, Zhang Z and Lu B, 2016. Development of exosome surface display technology in living human cells. Biochemical and Biophysical Research Communications,. 472, pp.53–59. [PubMed: 26902116]
12. Wen SW, Sceneay J, Lima LG, Wong CS, Becker M, Krumeich S, Lobb RJ, Castillo V, Wong KN, Ellis S, Parker BS and Moller A, 2016. The biodistribution and immune suppressive effects of breast cancer-derived exosomes. Cancer Research,. 76, pp.6816–6827. [PubMed: 27760789]

13. Jang SC, Kim SR, Yoon YJ, Park KS, Kim JH, Lee J, Kim OY, Choi EJ, Kim DK, Choi DS, Kim YK, Park J, Di Vizio D and Gho YS, 2015. In vivo kinetic biodistribution of nano-sized outer membrane vesicles derived from bacteria. Small,. 11, pp.456–461. [PubMed: 25196673]

14. Watson DC, Bayik D, Srivatsan A, Bergamaschi C, Valentin A, Niu G, Bear J, Monninger M, Sun M, Morales-Kastresana A, Jones JC, Felber BK, Chen X, Gursel I and Pavlakis GN, 2016. Efficient production and enhanced tumor delivery of engineered extracellular vesicles. Biomaterials,. 105, pp.195–205. [PubMed: 27522254]

15. Smyth T, Kullberg M, Malik N, Smith-Jones P, Graner MW and Anchordoquy TJ, 2015. Biodistribution and delivery efficiency of unmodified tumor-derived exosomes. Journal of Controlled Release,. 199, pp.145–155. [PubMed: 25523519]

16. Patel MM and Patel BM, 2017. Crossing the blood-brain barrier: Recent advances in drug delivery to the brain. CNS Drugs.

17. Li X, Tsibouklis J, Weng T, Zhang B, Yin G, Feng G, Cui Y, Savina IN, Mikhalovska LI, Sandeman SR, Howel CA and Mikhalovsky SV, 2016. Nano carriers for drug transport across the blood-brain barrier. Journal of Drug Targeting, pp.1–12.

18. Jones RM and Hynynen K, 2019. Advances in acoustic monitoring and control of focused ultrasound-mediated increases in blood-brain barrier permeability. British Journal of Radiology,. 92, p.20180601. [PubMed: 30507302]

19. Abrahao A, Meng Y, Llinas M, Huang Y, Hamani C, Mainprize T, Aubert I, Heyn C, Black SE, Hynynen K, Lipsman N and Zinman L, 2019. First-in-human trial of blood-brain barrier opening in amyotrophic lateral sclerosis using MR-guided focused ultrasound. Nature Communications,. 10, p.4373.

20. Hynynen K, Mcdannold N, Vykhodtseva N and Jolesz FA, 2001. Noninvasive MR imaging-guided focal opening of the blood-brain barrier in rabbits. Radiology,. 220,. pp.640–646. [PubMed: 11526261]

21. Sheikov N, Mcdannold N, Vykhodtseva N, Jolesz F and Hynynen K, 2004. Cellular mechanisms of the blood-brain barrier opening induced by ultrasound in presence of microbubbles. Ultrasound in Medicine and Biology,. 30, pp.979–989. [PubMed: 15313330]

22. Mesiwala AH, Farrell L, Wenzel HJ, Silbergeld DL, Crum LA, Winn HR and Mourad PD, 2002. High-intensity focused ultrasound selectively disrupts the blood-brain barrier in vivo. Ultrasound in Medicine and Biology,. 28,. pp.389–400. [PubMed: 11978420]

23. Hynynen K, Mcdannold N, Vykhodtseva N, Raymond S, Weissleder R, Jolesz FA and Sheikov N, 2006. Focal disruption of the blood-brain barrier due to 260-kHz ultrasound bursts: A method for molecular imaging and targeted drug delivery. Journal of Neurosurgery,. 105, pp.445–454. [PubMed: 16961141]

24. Fan CH, Liu HL, Ting CY, Lee YH, Huang CY, Ma YJ, Wei KC, Yen TC and Yeh CK, 2014. Submicron-bubble-enhanced focused ultrasound for blood-brain barrier disruption and improved CNS drug delivery. PloS One,. 9, p.e96327. [PubMed: 24788566]

25. Nisbet RM, Van Der Jeugd A, Leinenga G, Evans HT, Janowicz PW and Gotz J, 2017. Combined effects of scanning ultrasound and a tau-specific single chain antibody in a tau transgenic mouse model. Brain,. 140, pp.1220–1230. [PubMed: 28379300]

26. Kovacs ZI, Kim S, Jikaria N, Qureshi F, Milo B, Lewis BK, Bresler M, Burks SR and Frank JA, 2017. Disrupting the blood-brain barrier by focused ultrasound induces sterile inflammation. Proceedings of the National Academy of Sciences of the United States of America,. 114, pp.e75–e84. [PubMed: 27994152]

27. Jordão JF, Ayala-Grosso CA, Markham K, Huang Y, Chopra R, Mclaurin J, Hynynen K and Aubert I, 2010. Antibodies targeted to the brain with image-guided focused ultrasound reduces amyloid-beta plaque load in the TgCRND8 mouse model of Alzheimer's disease. PloS One,. 5, p.e10549. [PubMed: 20485502]

28. Anderson SA, Glod J, Arbab AS, Noel M, Ashari P, Fine HA and Frank JA, 2005. Noninvasive MR imaging of magnetically labeled stem cells to directly identify neovasculature in a glioma model. Blood,. 105, pp.420–425. [PubMed: 15331444]

29. Samiotaki G and Konofagou EE, 2013. Dependence of the reversibility of focused-ultrasound-induced blood-brain barrier opening on pressure and pulse length in vivo. IEEE transactions on ultrasonics. Ferroelectrics, and Frequency Control,. 60, pp.2257–2265. [PubMed: 24158283]
30. Hynynen K, Mcdannold N, Sheikov NA, Jolesz FA and Vykhodtseva N, 2005. Local and reversible blood-brain barrier disruption by noninvasive focused ultrasound at frequencies suitable for trans-skull sonications. NeuroImage,. 24, pp.12–20. [PubMed: 15588592]
31. Marquet F, Tung YS, Teichert T, Ferrera VP and Konofagou EE, 2011. Noninvasive, transient and selective blood-brain barrier opening in non-human primates in vivo. PloS One,. 6, p.e22598. [PubMed: 21799913]
32. Konofagou EE, Tung YS, Choi J, Deffieux T, Baseri B and Vlachos F, 2012. Ultrasound-induced blood-brain barrier opening. Current Pharmaceutical Biotechnology,. 13, pp.1332–1345. [PubMed: 22201586]
33. Burgess A, Ayala-Grosso CA, Ganguly M, Jordao JF, Aubert I and Hynynen K, 2011. Targeted delivery of neural stem cells to the brain using MRI-guided focused ultrasound to disrupt the blood-brain barrier. PloS One,. 6, p.e27877. [PubMed: 22114718]
34. Aryal M, Fischer K, Gentile C, Gitto S, Zhang YZ and Mcdannold N, 2017. Effects on P-glycoprotein expression after blood-brain barrier disruption using focused ultrasound and microbubbles. PloS One,. 12, p.e0166061. [PubMed: 28045902]
35. Jordão JF, Thévenot E, Markham-Coultes K, Scarcelli T, Weng YQ, Xhima K, O'reilly M, Huang Y, Mclaurin J, Hynynen K and Aubert I, 2013. Amyloid-β plaque reduction, endogenous antibody delivery and glial activation by brain-targeted, transcranial focused ultrasound. Experimental Neurology,. 248, pp.16–29. [PubMed: 23707300]
36. Liu HL, Hua MY, Yang HW, Huang CY, Chu PC, Wu JS, Tseng IC, Wang JJ, Yen TC, Chen PY and Wei KC, 2010. Magnetic resonance monitoring of focused ultrasound/magnetic nanoparticle targeting delivery of therapeutic agents to the brain. Proceedings of the National Academy of Sciences of the United States of America,. 107, pp.15205–15210. [PubMed: 20696897]
37. Hsu PH, Wei KC, Huang CY, Wen CJ, Yen TC, Liu CL, Lin YT, Chen JC, Shen CR and Liu HL, 2013. Noninvasive and targeted gene delivery into the brain using microbubble-facilitated focused ultrasound. PloS One,. 8, p.e57682. [PubMed: 23460893]
38. Choi JJ, Pernot M, Brown TR, Small SA and Konofagou EE, 2007. Spatio-temporal analysis of molecular delivery through the blood-brain barrier using focused ultrasound. Physics in Medicine and Biology,. 52, pp.5509–5530. [PubMed: 17804879]
39. Kovacs ZI, Tu T-W, Sundby M, Qureshi F, Lewis BK, Jikaria N, Burks SR and Frank JA, 2018. MRI and histological evaluation of pulsed focused ultrasound and microbubbles treatment effects in the brain. Theranostics,. 8, pp.4837–4855. [PubMed: 30279741]
40. Rashid MH, Borin TF, Ara R, Angara K, Cai J, Achyut BR, Liu Y and Arbab AS, 2019. Differential in vivo biodistribution of (131)I-labeled exosomes from diverse cellular origins and its implication for theranostic application. Nanomedicine: Nanotechnology Biology, and Medicine,. 21, p.102072. [PubMed: 31376572]
41. Frank JA, Kalish H, Jordan EK, Anderson SA, Pawelczyk E and Arbab AS, 2007. Color transformation and fluorescence of prussian blue-positive cells: Implications for histologic verification of cells labeled with superparamagnetic iron oxide nanoparticles. Molecular Imaging,. 6, pp.212–218. [PubMed: 17532887]
42. Zhang Z, Chopp M, Zhang RL and Goussev A, 1997. A mouse model of embolic focal cerebral ischemia. Journal of Cerebral Blood Flow and Metabolism,. 17, pp.1081–1088. [PubMed: 9346433]
43. Khan MB, Hoda MN, Vaibhav K, Giri S, Wang P, Waller JL, Ergul A, Dhandapani KM, Fagan SC and Hess DC, 2015. Remote ischemic postconditioning: Harnessing endogenous protection in a murine model of vascular cognitive impairment. Translational Stroke Research,. 6, pp.69–77. [PubMed: 25351177]
44. Saunders NR, Dziegielewska KM, Mollgard K and Habgood MD, 2015. Markers for blood-brain barrier integrity: How appropriate is evans blue in the twenty-first century and what are the alternatives? Frontiers in Neuroscience,. 9, p.385. [PubMed: 26578854]

45. Webb RL, Kaiser EE, Scoville SL, Thompson TA, Fatima S, Pandya C, Sriram K, Swetenburg RL, Vaibhav K, Arbab AS, Baban B, Dhandapani KM, Hess DC, Hoda MN and Stice SL, 2018. Human neural stem cell extracellular vesicles improve tissue and functional recovery in the murine thromboembolic stroke model. Translational Stroke Research,. 9, pp.530–539. [PubMed: 29285679]
46. Chen KT, Wei KC and Liu HL, 2019. Theranostic strategy of focused ultrasound induced blood-brain barrier opening for CNS disease treatment. Frontiers in Pharmacology,. 10, p.86. [PubMed: 30792657]
47. Hersh DS, Anastasiadis P, Mohammadabadi A, Nguyen BA, Guo S, Winkles JA, Kim AJ, Gullapalli R, Keller A, Frenkel V and Woodworth GF, 2018. MR-Guided transcranial focused ultrasound safely enhances interstitial dispersion of large polymeric nanoparticles in the living brain. PloS One,. 13, p.e0192240. [PubMed: 29415084]
48. Yang Y and Rosenberg GA, 2011. Blood-brain barrier breakdown in acute and chronic cerebrovascular disease. Stroke,. 42, pp.3323–3328. [PubMed: 21940972]
49. Gelderblom M, Leypoldt F, Steinbach K, Behrens D, Choe CU, Siler DA, Arumugam TV, Orthey E, Gerloff C, Tolosa E and Magnus T, 2009. Temporal and spatial dynamics of cerebral immune cell accumulation in stroke. Stroke,. 40, pp.1849–1857. [PubMed: 19265055]
50. George PM and Steinberg GK, 2015. Novel stroke therapeutics: Unraveling stroke pathophysiology and Its impact on clinical treatments. Neuron,. 87, pp.297–309. [PubMed: 26182415]
51. Doeppner TR, Herz J, GÖrgens A, Schlechter J, Ludwig AK, Radtke S, De Miroschedji K, Horn PA, Giebel B and Hermann DM, 2015. Extracellular vesicles improve post-stroke neuroregeneration and prevent postischemic immunosuppression. STEM CELLS Translational Medicine,. 4, pp.1131–1143. [PubMed: 26339036]
52. Otero-Ortega L, Laso-Garcia F, Gomez-De Frutos MD, Rodriguez-Frutos B, Pascual-Guerra J, Fuentes B, Diez-Tejedor E and Gutierrez-Fernandez M, 2017. White matter repair after extracellular vesicles administration in an experimental animal model of subcortical stroke. Scientific Reports,. 7, p.44433. [PubMed: 28300134]
53. Pardridge WM, 2005. The blood-brain barrier: Bottleneck in brain drug development. NeuroRx,. 2, pp.3–14. [PubMed: 15717053]
54. Lipsman N, Meng Y, Bethune AJ, Huang Y, Lam B, Masellis M, Herrmann N, Heyn C, Aubert I, Boutet A, Smith GS, Hynynen K and Black SE, 2018. Blood-brain barrier opening in Alzheimer's disease using MR-guided focused ultrasound. Nature Communications,. 9, p.2336.
55. Mainprize T, Lipsman N, Huang Y, Meng Y, Bethune A, Ironside S, Heyn C, Alkins R, Trudeau M, Sahgal A, Perry J and Hynynen K, 2019. Blood-brain barrier opening in primary brain tumors with non-invasive MR-guided focused ultrasound: A clinical safety and feasibility study. Scientific Reports,. 9, p.321. [PubMed: 30674905]
56. Arif WM, Elsinga PH, Gasca-Salas C, Versluis M, Martinez-Fernandez R, Dierckx R, Borra RJH and Luurtsema G, 2020. Focused ultrasound for opening blood-brain barrier and drug delivery monitored with positron emission tomography. Journal of Controlled Release,. 324, pp.303–316. [PubMed: 32428519]
57. Alexandrov AV, KÖhrmann M, Soinne L, Tsivgoulis G, Barreto AD, Demchuk AM, Sharma VK, Mikulik R, Muir KW, Brandt G, Alleman J, Grotta JC, Levi CR, Molina CA, Saqqur M, Mavridis D, Psaltopoulou T, Vosko M, Fiebach JB, Mandava P, Kent TA, Alexandrov AW and Schellinger PD, 2019. Safety and efficacy of sonothrombolysis for acute ischaemic stroke: A multicentre, double-blind, phase 3, randomised controlled trial. Lancet Neurology,. 18, pp.338–347. [PubMed: 30878103]
58. Mohammadabadi A, Huynh RN, Wadajkar AS, Lapidus RG, Kim AJ, Raub CB and Frenkel V, 2020. Pulsed focused ultrasound lowers interstitial fluid pressure and increases nanoparticle delivery and penetration in head and neck squamous cell carcinoma xenograft tumors. Physics in Medicine and Biology,. 65, p.125017. [PubMed: 32460260]
59. Mcdannold N, King RL and Hynynen K, 2004. MRI monitoring of heating produced by ultrasound absorption in the skull: In vivo study in pigs. Magnetic Resonance in Medicine,. 51, pp.1061–1065. [PubMed: 15122691]

60. Naor O, Krupa S and Shoham S, 2016. Ultrasonic neuromodulation. Journal of Neural Engineering,. 13, p.031003.

Health Research Alliance Author Manuscript

Health Research Alliance Author Manuscript

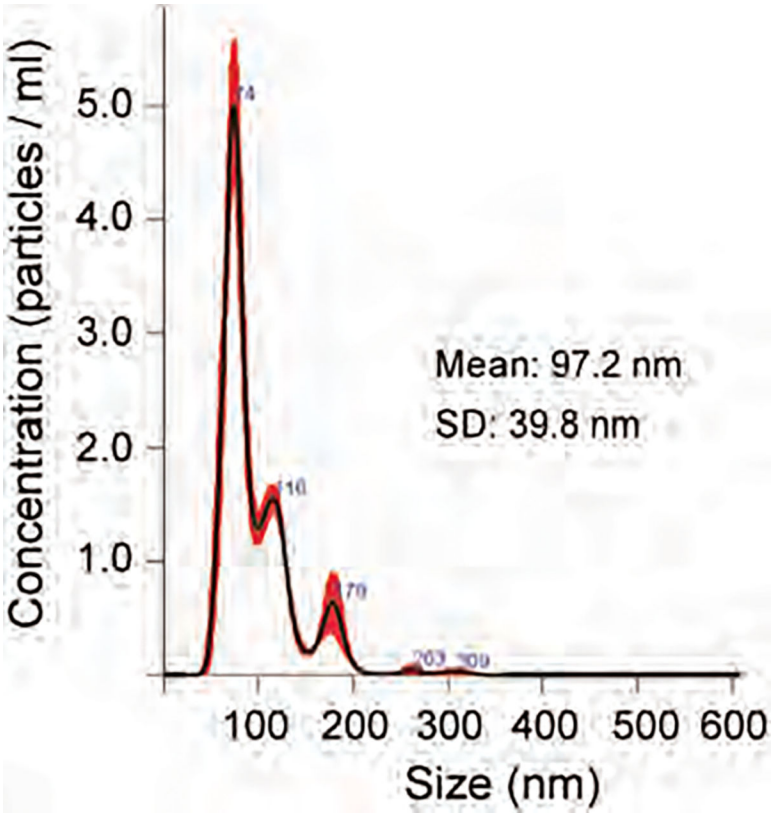

Figure 1.
Size distribution of EPC exosomes.

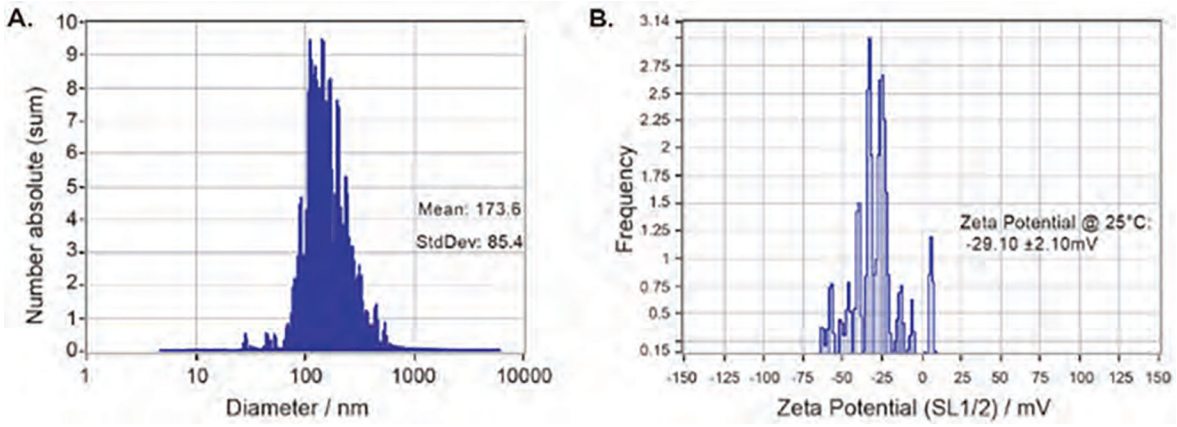

Figure 2.
NTA analysis of nanobubble's size (A) and zeta potential (B).

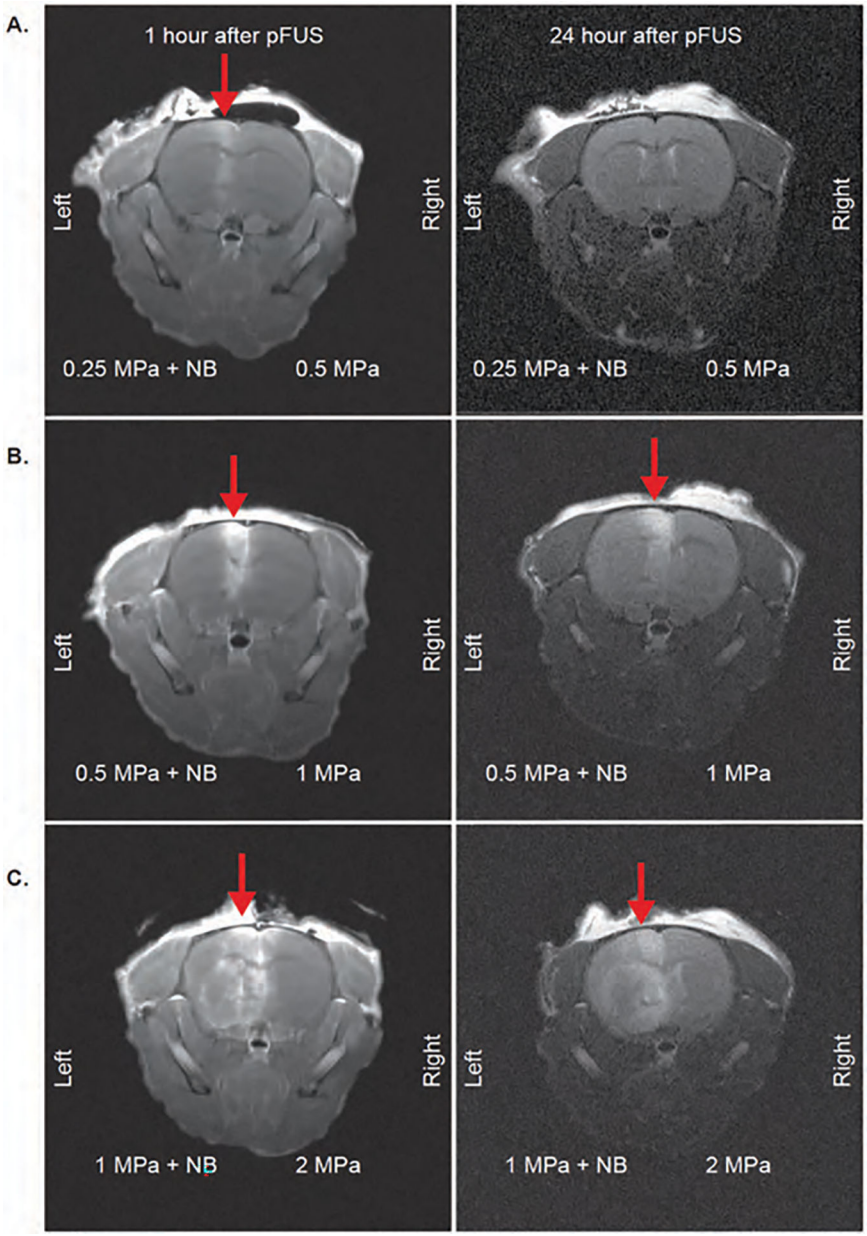

Figure 3.

Post-contrast T1 images to evaluate BBB opening of mice brains with pFUS application. 1 hour and 24 hour MRI images of mice with 0.25 MPa + NB to left hemisphere, 0.5 MPa to right hemisphere (A); 0.5 MPa + NB to left hemisphere, 1 MPa to the right hemisphere (B); 1 MPa + NB to left hemisphere, 2 MPa to the right hemisphere (C). Red arrows indicate leakage from BBB.

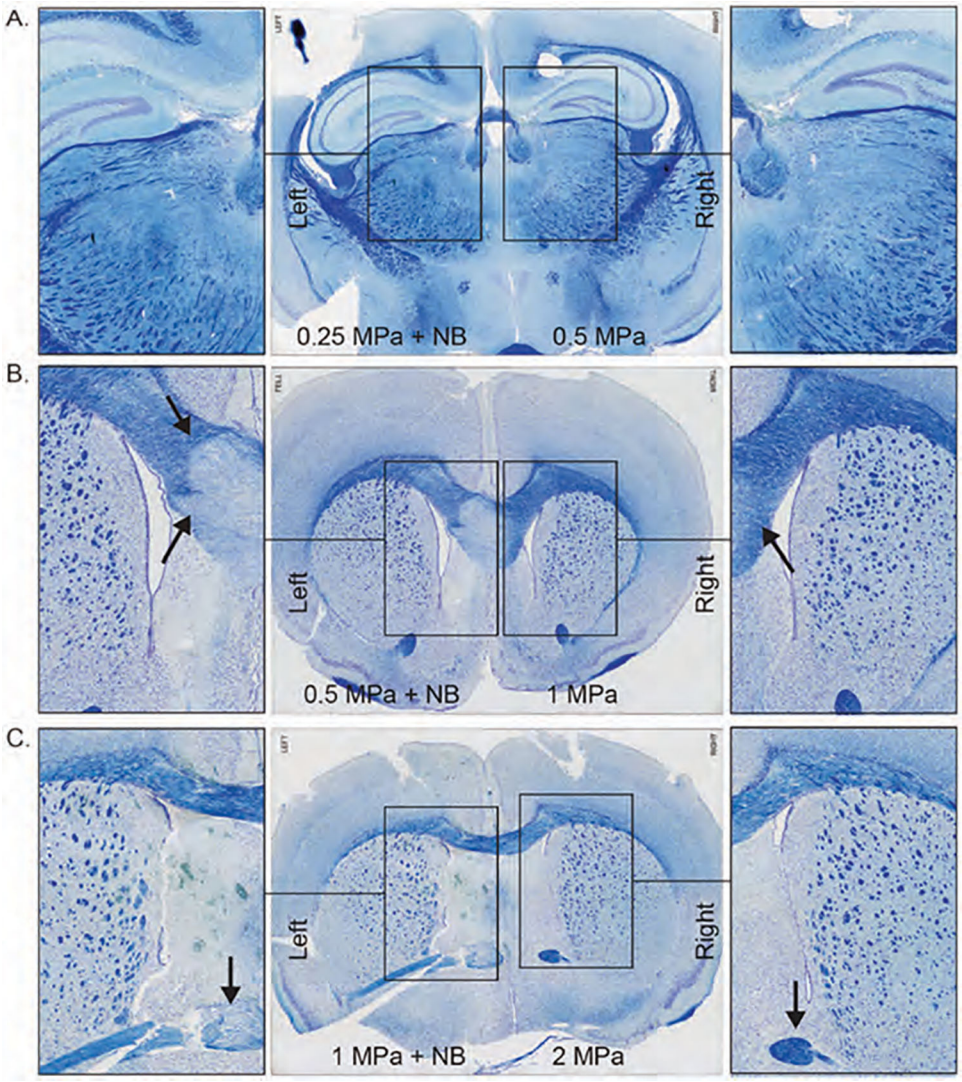

Figure 4.

Luxol Fast Blue staining of pFUS applied mice brain with 0.25 MPa + NB to left hemisphere, 0.5 MPa to the right hemisphere (A); 0.5 MPa + NB to left hemisphere, 1 MPa to the right hemisphere (B); 1 MPa + NB to left hemisphere, 2 MPa to the right hemisphere (C).

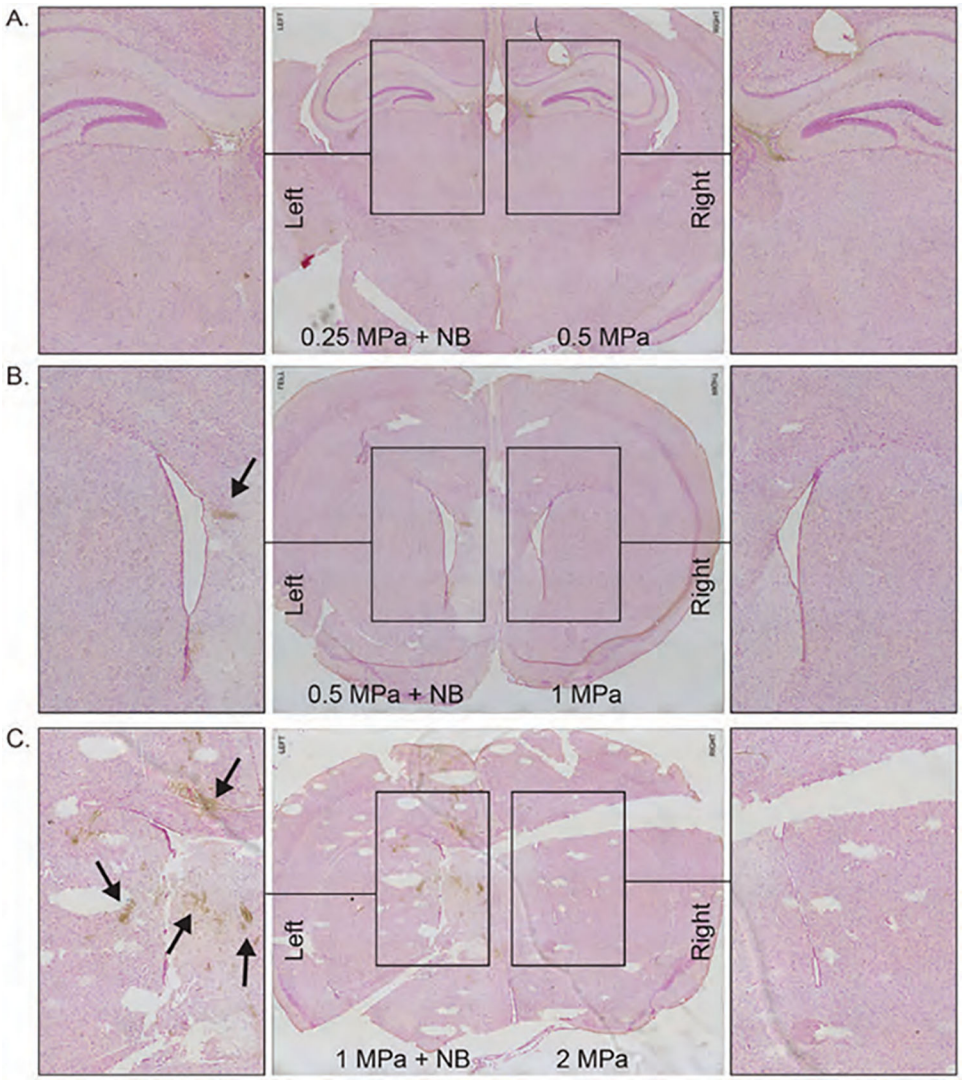

Figure 5.

Prussian Blue staining of pFUS applied mice brain with 0.25 MPa + NB to left hemisphere, 0.5 MPa to the right hemisphere (A); 0.5 MPa + NB to left hemisphere, 1 MPa to the right hemisphere (B); 1 MPa + NB to left hemisphere, 2 MPa to the right hemisphere (C). Arrows indicate hemosiderin stained with Prussian blue.

Health Research Alliance Author Manuscript

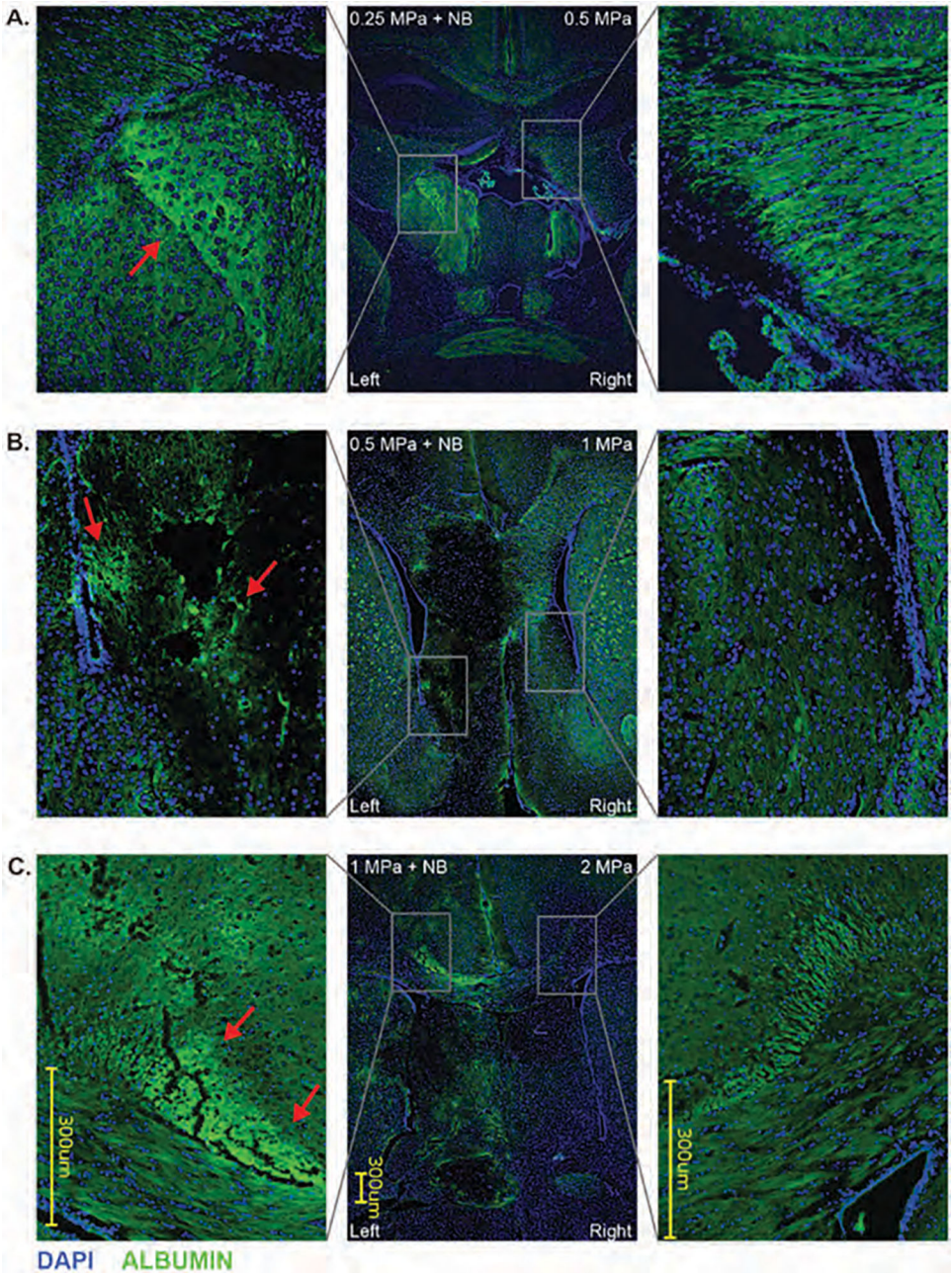

Figure 6.

Albumin and DAPI immunofluorescence labeling of pFUS applied mice brain with 0.25 MPa + NB to left hemisphere, 0.5 MPa to the right hemisphere (A); 0.5 MPa + NB to left hemisphere, 1 MPa to the right hemisphere (B); 1 MPa + NB to left hemisphere, 2 MPa to the right hemisphere (C). Arrows indicate fluorescent-labeled albumin.

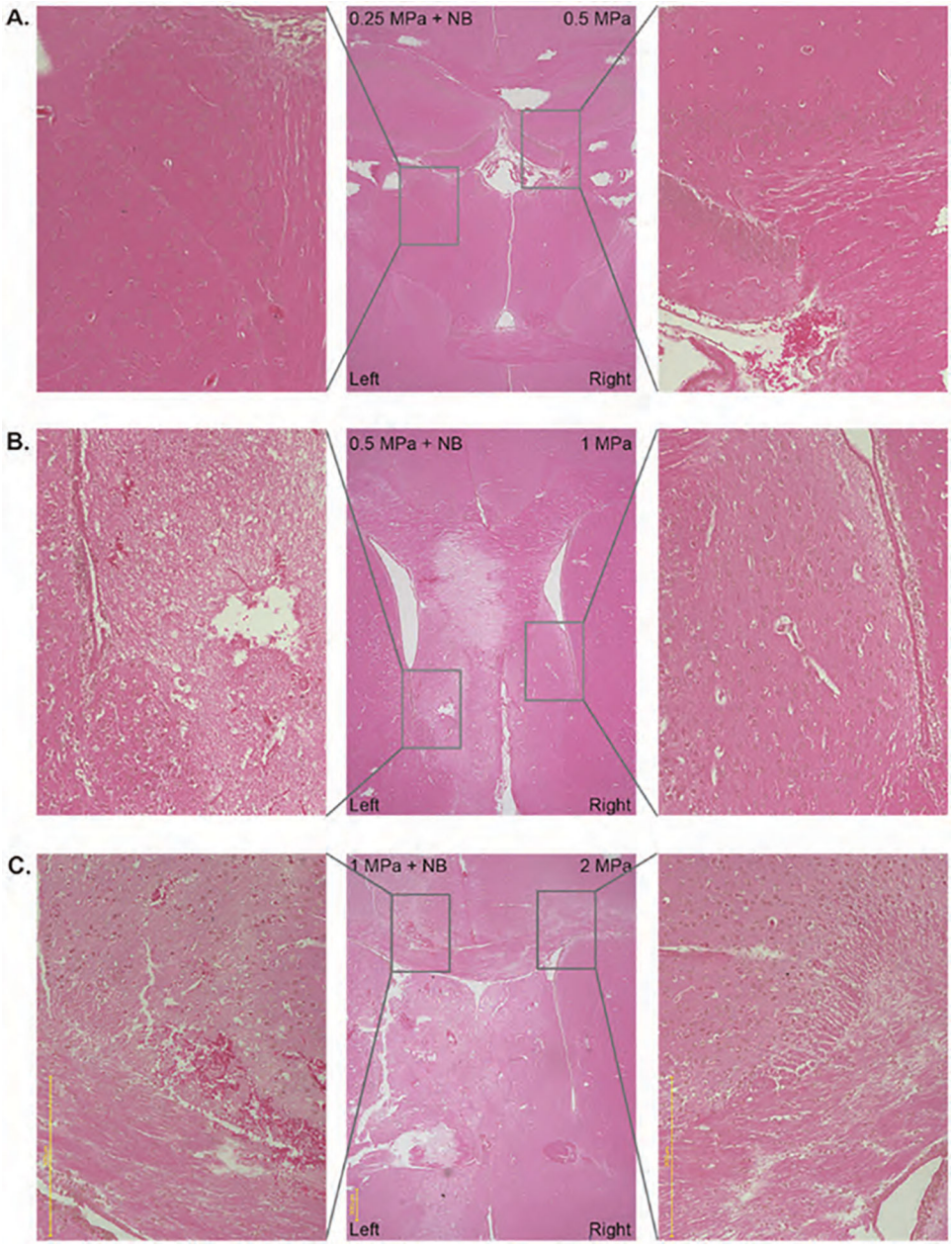

Figure 7.

Hematoxylin and eosin staining of pFUS applied mice brain with 0.25 MPa + NB to left hemisphere, 0.5 MPa to the right hemisphere (A); 0.5 MPa + NB to left hemisphere, 1 MPa to the right hemisphere (B); 1 MPa + NB to left hemisphere, 2 MPa to the right hemisphere (C).

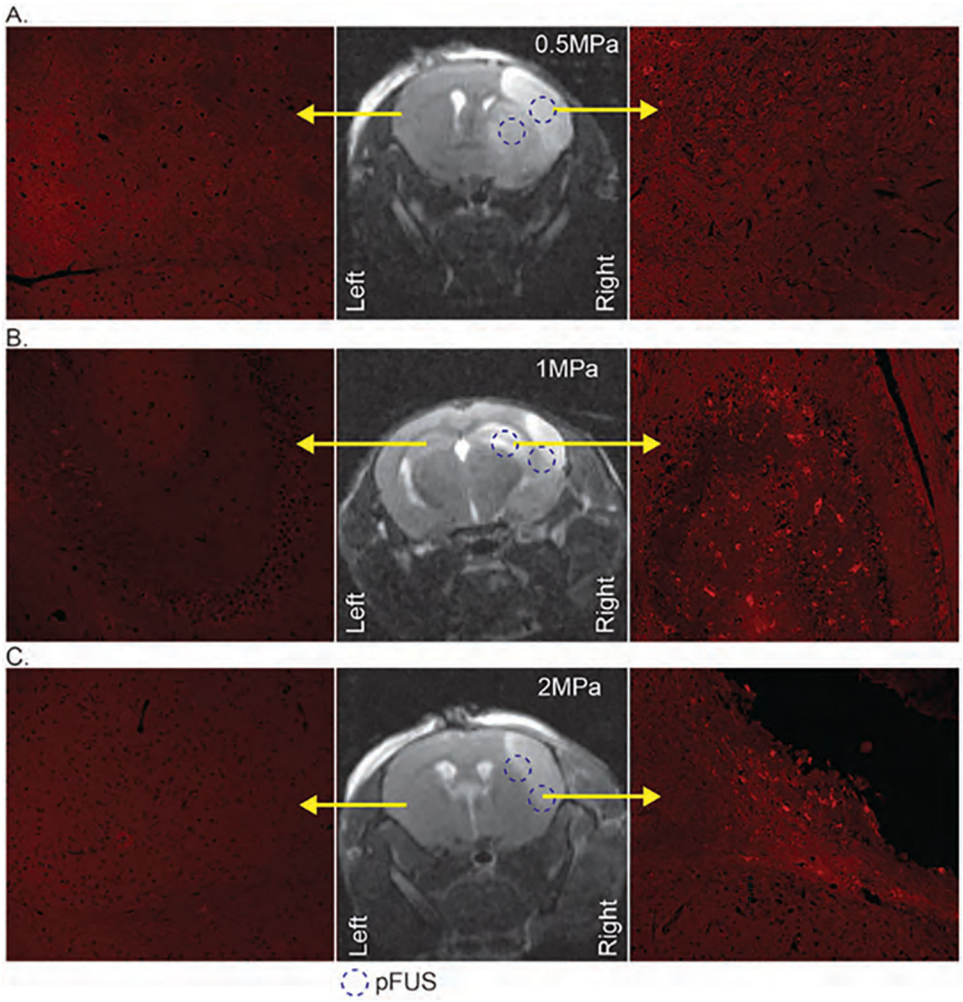

Figure 8.

MRI images (middle column) to indicate the stroke area of mice and dotted circle to delineate the 2 pFUS application points. The right column with fluorescent microscopy images to show DiI-labeled (red) exosomes from the right hemisphere of the mice with 0.5 MPa (A), 1 MPa (B), and 2 MPa (C) pFUS application; left columns with fluorescent microscopy images to show the contralateral side of the brain without stroke and pFUS application.

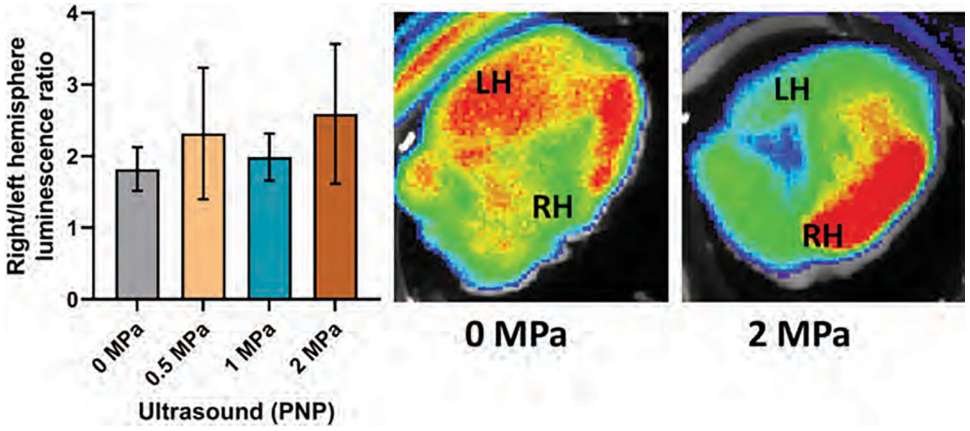

Figure 9.

Photon intensity ratio of the right hemisphere to left hemisphere of the mouse brain with stroke and representative fluorescent images of *ex vivo* brain. ($n = 4$).

Health Research Alliance Author Manuscript

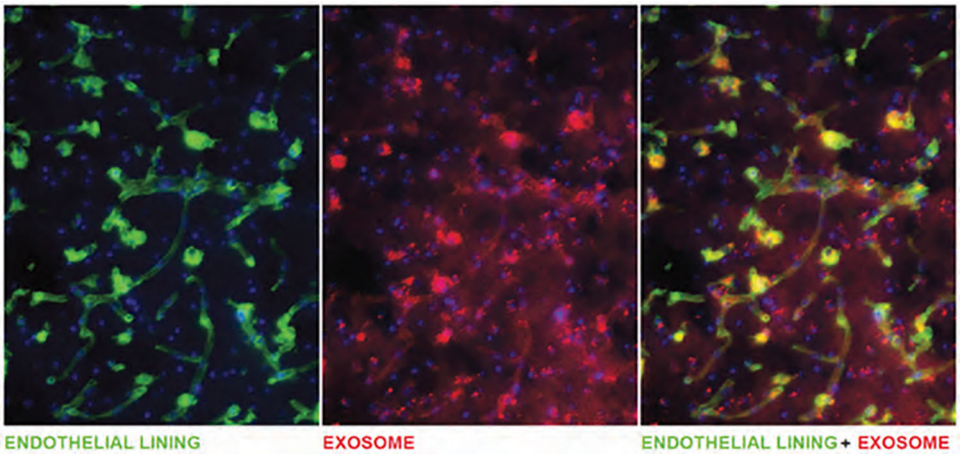

Figure 10.

Fluorescent image of FITC-labeled Lectin delineates endothelial lining of vessels and DiI positive exosomes.

Table I.

Previous ultrasound studies and parameters to open BBB.

Reference	Organism	Pressure (MPa)	Frequency (MHz)	Burst rate (Hz)	Burst (ms)	Duration (second)
[21]	Rabbit	1	1.5–1.63	1	100	20
[29]	Mice	0.3	1.5	10	6.7	60
[30]	Rabbit	0.4	0.69	1	10	20
[31]	Primates	0.3	0.5	2	10	120
[24]	Rats	0.2	1	10		60
[32]	Mouse	0.3	1.5	10	20	60
[33]	Rats	0.24	0.558	1	1	120
[34]	Rats	0.55	0.4–1.7	1	10	60
[35]	Mice	0.3	0.5	1	10	120
[36]	Rats	0.62	0.4	1	10	120
[27]	Mice	0.3	0.558	1	10	120
[37]	Mice	0.44	1.5	1	10	120
[38]	Mice	0.67	1.525	10	20	30
[39]	Rats	0.3	0.548	0.5–0.6	10	120
[26]	Rats	0.3	0.590	1	10	120